

Ground-State Parameters for the Quasi-Two-Dimensional Close-Packed He⁴ Solid at High Density*

Anthony D. Novaco

Brookhaven National Laboratory, Upton, New York 11973

(Received 2 July 1973)

A theoretical calculation of the chemical potential, spreading pressure, and inverse compressibility at 0°K is reported for He⁴ adsorbed on a graphite-like substrate for monolayer densities of 0.10 to 0.13 Å⁻². These functions are obtained from a ground-state variational wave function constructed of single-particle functions multiplied by Jastrow correlation factors. Use was made of a cluster expansion in the calculation of the ground-state energy. The theoretical results agree quite well with the empirical values.

I. INTRODUCTION

The current wisdom regarding the adsorbed helium monolayer film is that for low enough temperatures and for areal densities near that of the completed monolayer, the film behaves as a highly compressed two-dimensional quantum solid.¹⁻³ The maximum density of the first layer (~0.115 Å⁻² for He⁴ adsorbed upon Grafoil) is essentially achieved at monolayer completion, at which point further addition of helium atoms to the film results in the formation of a second layer of adatoms with negligible further compression of the first.⁴ This behavior seems to be typical of adsorption of helium upon a variety of solid substrates.

A recently published calculation of the ground-state properties of the helium monolayer used the Hartree approximation to calculate such properties as the density of monolayer completion, Debye temperature, Debye-Waller factor, and structure factor.³ Using a semiempirical potential for the helium-helium interaction, and neglecting the effect of adatom zero-point motion normal to the surface upon the lateral interaction, the calculation produced results in reasonable agreement with experiment. No results were reported for the spreading pressure or compressibility.

Since the publication of that calculation, more extensive empirical information has become available.^{5,6} In particular, the compressibility at 4.2°K has been measured and the chemical potential at 0°K has been empirically determined—both of these parameters were determined for helium adsorbed upon the substrate Grafoil. It is thus appropriate to examine in a quantitative manner some specific questions regarding the high-density helium monolayer. For example,

how important to the thermodynamics of the monolayer is the vibrational softening of the lateral helium-helium interaction due to zero-point oscillations perpendicular to the surface? Is there any significant coupling between lateral and normal zero-point oscillations? Furthermore, what specific role does the substrate play and does the periodic structure of the substrate surface influence the structure of the monolayer film at high density? Finally, it would be useful to shed some light upon the extent to which the bare helium-helium potential is modified by the presence of the substrate.

The calculation reported here is that of the chemical potential, spreading pressure, and compressibility at 0°K as functions of areal density ρ in the range $0.10 \leq \rho \leq 0.13 \text{ \AA}^{-2}$. These functions are calculated from a ground-state energy derived from a variational wave function which describes a quasi-two-dimensional close-packed lattice of helium atoms. In this calculation, the effects of both zero-point motion normal to the surface and lateral correlations are examined, although the zero-point oscillations normal to the plane are “decoupled” from the lateral zero-point oscillations. In this manner, the variational problem is separated into an effectively two-dimensional one and an effectively one-dimensional one.

The philosophy of this calculation is to obtain good quantitative estimates of the important physics of the monolayer beyond the simple two-dimensional Hartree approximation. However, no attempt was made to do a final state-of-the-art calculation. Instead, the goal was to elicit results which have the same confidence level as experiment (~10%), as judged by some reasonable criterion.

II. VARIATIONAL CALCULATION

The Hamiltonian \hat{H} chosen for the adatom-substrate system describes the substrate as an ideal and rigid lattice of carbon atoms with the graphite crystal structure. The substrate is assumed to be a semi-infinite solid with a basal plane surface. The helium-graphite interaction is represented by a static potential $U(\vec{r}, z)$, where \vec{r} is the lateral position vector of the adatom and z is its normal coordinate. The calculation of $U(\vec{r}, z)$ as a sum of two-body potentials is described in Ref. (7), Appendix A. The helium-helium interaction is described by the Beck potential, as this form seems to be about the best of the semiempirical potentials which have been used to describe the interaction of two helium atoms in vacuum.^{8,9} The assumption is that substrate-mediated effects^{10,11} are unimportant in the high-density region. The Hamiltonian is then

$$\hat{H} = \sum_j \left[-\frac{\hbar^2}{2M} \left(\nabla_j^2 + \frac{\partial^2}{\partial z_j^2} \right) + U(\vec{r}_j, z_j) \right] + \sum_{i < j} v(\eta_{ij}), \quad (1)$$

where v is the Beck potential and $\eta_{ij}^2 = r_{ij}^2 + z_{ij}^2$. The trial wave function is written as a product of single-particle functions (which describe the z -wise localization and the lateral configuration) multiplied by a product of Jastrow factors which describe the lateral correlations. Therefore,

$$\Psi(\vec{r}_1, z_1, \dots, \vec{r}_N, z_N) = \prod_i \phi_i(\vec{r}_i, z_i) \prod_{j < i} f(r_{ji}). \quad (2)$$

The function ϕ_i is written as a separable function in the normal and lateral coordinates⁷:

$$\phi_i(\vec{r}_i, z_i) = (A/2\pi)^{1/2} e^{-A(\vec{r}_i - \vec{R}_i)^2/4} \sum_{\nu} C^{\nu} M^{\nu}(z_i), \quad (3)$$

where the \vec{R} are the direct lattice vectors for a two-dimensional hexagonal lattice, the $\{M^{\nu}\}$ are a suitably chosen orthonormal set of basis functions, and the parameters A and C^{ν} are determined variationally.

The variation of the correlation function $f(r)$ was restricted to a given functional form having variational parameters. This form was chosen in such a way that it is capable of reproducing the typical t -matrix function used in bulk-solid studies.¹² The form of $f(r)$ was constrained so as to satisfy (in the $r \rightarrow 0$ limit) the one-dimen-

sional Schrödinger equation for two helium atoms with an interaction given by the Beck potential. This is, of course, just the WKB form $f(r) = e^{-u(r)}$, with $u(r)$ given by¹³

$$u(r) = (-1/\hbar) \int dr [M \tilde{v}(r)]^{1/2}. \quad (4)$$

The form of $f(r)$ for finite r was modified by use of Padé approximants so that $f(r)$ is given by

$$f(r) = e^{-u(r)(1+P_1 r)/(Q_0 + Q_1 r)}. \quad (5)$$

In general, P_1 , Q_0 , and Q_1 can be treated as variational parameters. For the purposes of the present calculation, Q_0 was set equal to unity, P_1 was set equal to -0.4 \AA^{-1} , and Q_1 was used as the sole variational parameter. The resulting shape for $f(r)$ gives a quite reasonable fit to the Glyde-Khanna¹² correlation factor if Q_1 is set equal to zero. In fact, $Q_1 = 0$ gives the energy minimum (Q_1 positive), with the results for finite Q_1 being quite near the Hartree results ($Q_1 \rightarrow \infty$) if Q_1 is larger than 1.0 \AA^{-1} .

The calculation of $E_0 = \langle \Psi | \hat{H} | \Psi \rangle$ is carried out via a cluster expansion truncated after the two-body term.^{7,14} The energy E_0 is given by $E_0 = E_{01U} + E_{01V} + E_{02V}$, where

$$E_{01U} = (-\hbar^2/2M) \sum_{j=1}^N \langle \phi_j | \nabla_j^2 | \phi_j \rangle, \quad (6)$$

$$E_{01V} = \sum_{j=1}^N \langle \phi_j | (-\hbar^2/2M) \frac{\partial^2}{\partial z_j^2} + \bar{U}(z_j) | \phi_j \rangle, \quad (7)$$

$$E_{02V} = \sum_{j < i} \frac{\langle \phi_j \phi_i | f_{ji}^2 V_{ji} | \phi_j \phi_i \rangle}{\langle \phi_j \phi_i | f_{ji}^2 | \phi_j \phi_i \rangle}, \quad (8)$$

$$f_{ji} = f(|\vec{r}_j - \vec{r}_i|), \quad (9)$$

$$V_{ji} = V(|\vec{r}_j - \vec{r}_i|), \quad (10)$$

$$V(r) \equiv v_{2D}(r) - (\hbar^2/2M) \nabla^2 \ln f(r).$$

In the preceding, two Ansätze are made to facilitate the evaluation of E_{01U} and E_{02V} . Because the close-packed lattice used to describe the film has no simple relation to the lattice structure of the surface, E_{01U} is evaluated by replacing $U(\vec{r}, z)$ by $\bar{U}(z)$, where

$$\bar{U}(z) \equiv \frac{1}{\Omega} \int_{\Omega} d\vec{r} U(\vec{r}, z), \quad (11)$$

with Ω being the unit-cell area. The tacit assumption is that the structure of the high-density solid is determined almost entirely by the helium-helium interaction and is nearly decoupled from the lateral structure of the surface. The mis-

match between the monolayer and surface structures results in some averaging of the substrate potential, and in Eq. (11) this averaging is taken to be random. The calculation of E_{02V} involves the calculation of

$$v_{2D}(r_{j1}) \equiv \int_{-\infty}^{\infty} dz_j dz_l M^2(z_j) v(\eta_{j1}) M^2(z_l), \quad (12)$$

where $M(z) \equiv \sum_{\nu} C^{\nu} M^{\nu}(z)$. The functions used for $M^{\nu}(z)$ are "Morse functions" that is, solutions to the one-dimensional Schrödinger equation for the adatom in a Morse potential. Appendix B of Ref. 7 gives the details of these functions and appropriate references.

Rather than actually do the integral in Eq. (12), a weighted average of v was used to evaluate v_{2D} . That is, v_{2D} was approximated by

$$v_{2D}(r) = \frac{1}{16} [5.5 v(r) + 6.0 v((r^2 + \sigma^2)^{1/2}) + 4.5 v((r^2 + 4\sigma^2)^{1/2})], \quad (13)$$

where σ is given by

$$\sigma^2 \equiv \int_{-\infty}^{\infty} dz M^2(z) [z^2 - \bar{z}^2], \quad (14)$$

$$\bar{z} \equiv \int_{-\infty}^{\infty} dz z M^2(z). \quad (15)$$

This approximation is equivalent to replacing $M^2(z)$ in Eq. (12) with a normalized parabola having a maximum at \bar{z} and zeros at $\bar{z} \pm 2\sigma$ (with the limits of integration now being from $\bar{z} - 2\sigma$ to $\bar{z} + 2\sigma$), and evaluating each line integral via a five-point Simpson's rule. Although Eq. (13) is only an approximation to Eq. (12), it contains all the important physics, namely, the softening of this lateral interaction v_{2D} due to the zero-point motion normal to the surface. The approximation was checked by comparing Eq. (13) to the actual numerical evaluation given in Eq. (12). This comparison showed that $v(r) - v_{2D}(r)$ was given to better than 5% by Eq. (13) for $1.0 < r < 2.5 \text{ \AA}$. For $r > 2.5 \text{ \AA}$, the approximation was accurate to a fraction of a degree.

The task is now to evaluate numerically E_0 for a given value of Q_1 , and to minimize E_0 as a function of A and the $\{C^{\nu}\}$. The value of E_0/N for optimum values of $\{A, C^{\nu}\}$ is denoted by $\epsilon(\rho)$, where ρ is the areal number density of the monolayer. For a given value of Q_1 , the term E_{01T} is solely a function of A , E_{01V} is solely a function of C^{ν} , while E_{02V} is a function of both A and C^{ν} . In minimizing E_0 , the variation of E_{02V} with C^{ν} is ignored so that the C^{ν} are determined by only minimizing E_{01V} . This set of C^{ν} is then used to calculate σ , and then $E_{01T} + E_{02V}$ are minimized with respect to A . This procedure decouples

lateral and normal vibrational modes, the assumption being that compressing the film in the lateral direction has no significant effect upon the amplitude of vibrations normal to the surface—at least not in the range of experimentally accessible densities. The calculation was repeated for several values of Q_1 in the range from 0 to 2.0 \AA^{-2} , and $Q_1 = 0$ always corresponded to the lowest value of E_0 .

In order to compare theory with experiment, the chemical potential μ , spreading pressure ϕ , and inverse compressibility K^{-1} were calculated from $\epsilon(\rho)$ using

$$\mu = \epsilon + \rho \frac{\partial \epsilon}{\partial \rho}, \quad (16)$$

$$\phi = \rho^2 \frac{\partial \epsilon}{\partial \rho}, \quad (17)$$

$$K^{-1} = 2\phi + \rho^3 \frac{\partial^2 \epsilon}{\partial \rho^2}. \quad (18)$$

Since each of the above parameters involves a different combination of $\epsilon(\rho)$ derivatives, both the general placement and shape of $\epsilon(\rho)$ can be examined.

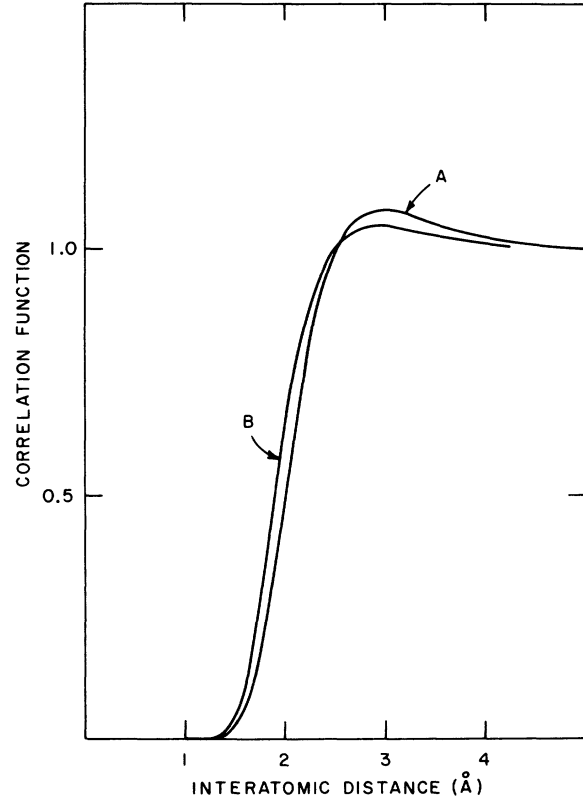


FIG. 1. Correlation function $f(r)$ with $Q_0 = 1.0$, $P_1 = -0.4 \text{ \AA}^{-1}$, and (A) $Q_1 = 0$ and (B) $Q_1 = 0.25 \text{ \AA}^{-1}$.

III. RESULTS

The cluster expansion for the Jastrow factor given by Eq. (5) has not been examined in detail, so that the rate of convergence (especially at high densities) is somewhat of an unknown for arbitrary values of the parameters P_1 , Q_0 , and Q_1 . However, for $Q_0 = 1.0$ and $P_1 = -0.4 \text{ \AA}^{-1}$, $f(r)$ has all the characteristics associated with rapid convergence of the expansion for bulk helium near the melting curve, and recent work by Brandow indicates the rate of convergence is not sensitive to reasonable changes in density.^{15,16} In particular, with Q_0 and P_1 fixed at the above values, $f(r)$ is similar in shape to other correlation functions for which E_{0sV} has been shown to be small.^{7,14,15} Furthermore, the two-dimensional nature of the monolayer means that there are simply fewer neighbors than in the bulk, so that the higher-order clusters will have smaller weight in two dimensions than in three. Finally, the correlated

results are not very different from the Hartree results, for which all higher terms vanish. Nevertheless, it is profitable to have some consistency check of the truncation error. This was done by comparing results for two correlation functions which can be expected to have some reasonable difference in convergence rates, but not so different that the exact variational results could be expected to differ drastically.

The one characteristic of $f(r)$ which does affect the rate of convergence is the deviation of $f(r)$ from unity for those values of r where the Gaussian factors assume large values.¹⁴⁻¹⁶ The two correlation functions are plotted in Fig. 1, function A being given by $f(r)$ with $Q_1 = 0$ and function B by $f(r)$ with $Q_1 = 0.25 \text{ \AA}^{-1}$. Function B differs from unity by about half the amount of function A in that region where the Gaussian factors have their largest values. It is just this property which should cause function B to be associated with a better convergence rate.¹⁵ Furthermore, the optimum Gaussian for function B was about 10% narrower than that for A, a property which also speeds the convergence rate. The energy

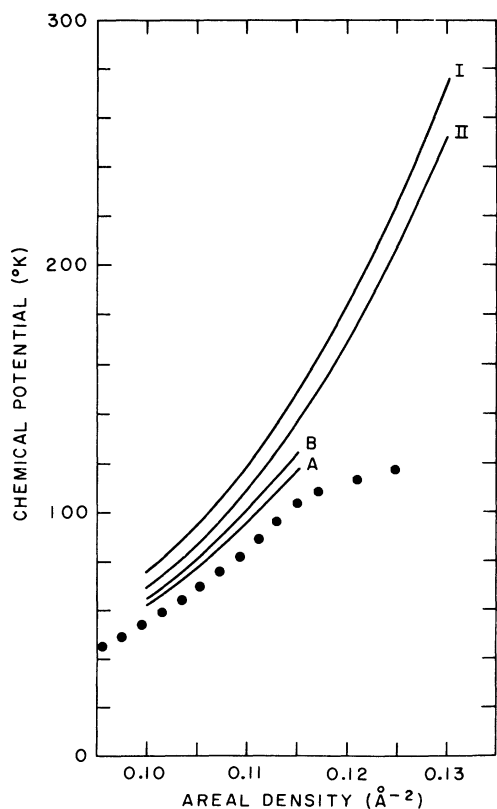


FIG. 2. Chemical potential at 0°K. (I) Two-dimensional Hartree; (II) quasi-two-dimensional Hartree; (A) quasi-two-dimensional cluster expansion using correlation function with $Q_1 = 0$; (B) same as (A) but using correlation function with $B_1 = 0.25 \text{ \AA}^{-1}$. The dots are empirical values (Ref. 5).

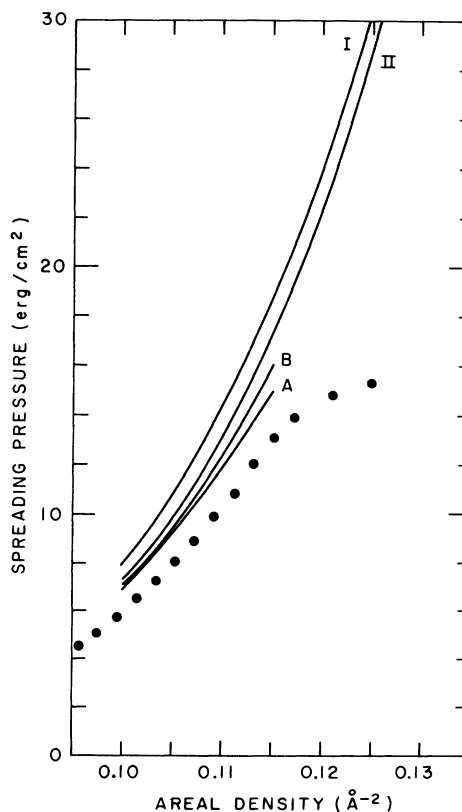


FIG. 3. Spreading pressure at 0°K. Curves I, II, A, and B are theoretical results using same notation as in Fig. 2. The dots are empirical values (Ref. 5).

values associated with A were always less by about 10% than those associated with B.

The theoretical results for μ , ϕ , and K^{-1} are plotted in Figs. 2-4, each graph displaying four theoretical curves. Curve I is the Hartree result [$f(r) \equiv 1$] for a strictly two-dimensional solid ($v_{2D} = v$). Curve II is also a Hartree result, but with v_{2D} calculated via Eq. (13). The difference between curves I and II shows the effects of normal vibrational motion upon the lateral interaction, and the concurrent effect upon the thermodynamic functions. Curves A and B are the theoretical results using correlation functions A and B, respectively, and again v_{2D} calculated via Eq. (13). The differences between these curves and curve II demonstrates the effects of correlations. The difference between curves A and B is small in each case, so no attempt was made to separate the contribution due to truncation and the difference due to better functional form. Rather, the small shift is evidence that the cluster results are consistent with higher-order corrections being small.

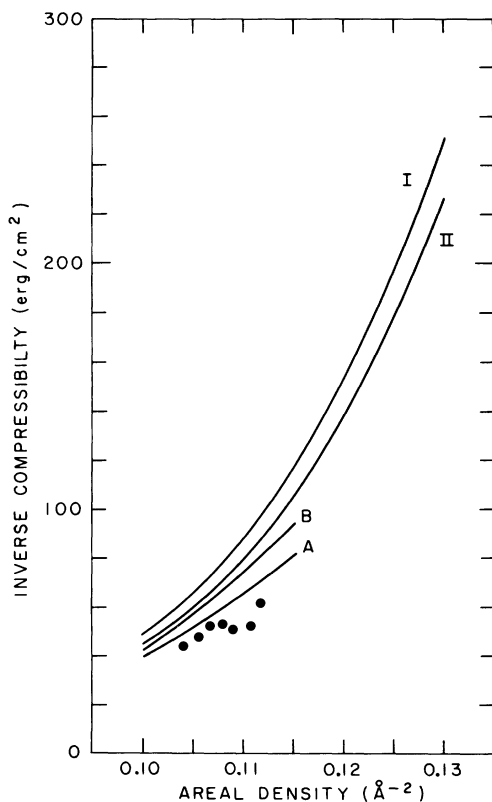


FIG. 4. Inverse compressibility. Curves I, II, A, and B are theoretical results at 0°K using the notation of Fig. 2. The dots are experimental results at 4.2°K (Ref. 6).

The experimental (or empirical) results for He⁴ adsorbed on Grafoil are shown as dots in Figs. 2-4. The empirical results of Elgin and Goodstein for the chemical potential at 0°K are shown in Fig. 2 shifted by their empirical binding energy of a single He⁴ atom on Grafoil (~145°K).⁵ Their 0°K result was obtained by numerical thermodynamic analysis of the finite ρ and T chemical potential and specific heats. The spreading pressure in Fig. 3 was calculated by integration of the Elgin and Goodstein chemical potential via

$$\phi(\rho) = \phi(\rho_0) - \rho_0 \mu(\rho_0) + \rho \mu(\rho) - \int_{\rho_0}^{\rho} d\rho' \mu(\rho'), \quad (19)$$

with ρ_0 taken at about 10^{-2} \AA^{-2} . In plotting $\phi(\rho)$ it has been assumed that $\phi(\rho_0) \ll \phi(\rho)$, and so $\phi(\rho_0)$ was ignored in Eq. (19). The inverse compressibility K^{-1} plotted in Fig. 4 is the measured result (at 4.2°K) of Stewart *et al.*⁶ This result is in good agreement with the result found by differentiating the chemical potential of Fig. 2. The dip in the experimental inverse compressibility at about 0.11 \AA^{-2} is apparently due to experimental error rather than any intrinsic structure.¹⁷ The "break" in the curves for μ and ϕ at 0.115 \AA^{-2} is due to monolayer completion.

The general agreement between theory and experiment is from about 10% for curve A to about 10 to 15% for curve B. The question as to the uncertainty to be associated with the experimental results is difficult, but one source of error is simply the measurement of the film density, with a reasonable estimate of this being about 1%.¹⁸ Another source of error would be lateral inhomogeneities causing a variation of film density from one region of the surface to another.⁵ A downward shift of about 1% in the experimental density would bring experimental results into excellent agreement with curve A. It was because the difference between curves A and B is less than the difference between curve A and experiment that no attempt was made to examine the effect of higher-order clusters.

IV. CONCLUSIONS

The chemical-potential and spreading-pressure results show that vibrational motion normal to the surface has as important an effect as lateral correlations, at least for monolayer densities within 15% of completion. The sum total of both effects—curve I vs curve A—is about 20% of the magnitude of μ and ϕ . However, this translates into only a 2% effect upon the density of monolayer completion. The major effect of lateral correlations on ϕ and μ is to lower the magnitude of each

by about 10% without much effect upon the density dependence. However, the effect of correlations on the density dependence of K^{-1} is quite notable since they are responsible for the rather flat density dependence of this parameter. The agreement between theory and experiment, especially with regard to K^{-1} , strongly indicates that there is no significant coupling between vibrational motion normal and lateral to the surface. That is, the film gives little indication of an instability normal to the surface as the film is compressed laterally. With a suitable substrate potential, this effect could be an important factor in determining the density and physics of monolayer completion.

The high density of the solid film considered rules out any hope of observing substrate-mediated effects on the bare helium-helium interaction unless these effects significantly affect the strongly repulsive region of that potential. One such possibility is the presence of electric fields at the surface, since this causes an additional dipole-dipole repulsion between the helium atoms. This effect has been discussed at length,¹⁹ and the contribution to the chemical potential is positive and additive in the classical limit. Since the data lie below the theory there is no evidence for the existence of such fields for the helium-Grafoil system. Nevertheless, it is useful to calculate a maximum value for such a field assuming some maximum contribution to μ . For the purposes of an order-of-magnitude estimate, it is sufficient to do the classical calculation for a simple hex-

agonal lattice neglecting depolarizing effects of nearby helium atoms. If $\Delta\mu$ is the contribution due to a uniform electric field generated by a surface charge σ , then

$$\Delta\mu = 20\pi^2 \alpha^2 \sigma^2 \sum_j \frac{\nu_j}{R_j^3}, \quad (20)$$

where α is the helium static polarizability, ν_j is the number of atoms in the j th nearest-neighbor shell, and R_j is the corresponding distance. If the value of $\Delta\mu$ is chosen (*ad hoc*) to be 10% of the total, then the excess charge per surface carbon atom is about 10^{-2} electrons. In fact, it is probable that these fields are zero.

The general agreement between theory and experiment leads to the conclusion that the main effect of the graphitelike substrates upon the physics of the high-density monolayer is simply to restrict the adatoms to a plane with small-amplitude zero-point oscillations about this plane. There is little, if any, effect upon μ , ϕ , and K^{-1} due to crystal surface structure, although this surface structure would probably effect the overall topological structure of the film. This behavior at high densities contrasts sharply with the superlattice phase, where the structure of the surface has a very important effect upon the basic structure and thermodynamics of the film.^{7,20}

ACKNOWLEDGMENT

I would like to thank V. J. Emery for helpful discussions.

*Work performed under the auspices of the U. S. Atomic Energy Commission.

¹F. D. Manchester, *Rev. Mod. Phys.* **39**, 383 (1967).

²J. G. Dash, *J. Low Temp. Phys.* **3**, 301 (1970).

³A. D. Novaco, *Phys. Rev. A* **7**, 678 (1973).

⁴C. E. Campbell, F. J. Milford, A. D. Novaco, and M. Schick, *Phys. Rev. A* **6**, 1648 (1972).

⁵R. L. Elgin and D. L. Goodstein, in *Proceedings of the Thirteenth International Conference on Low Temperature Physics*, Boulder, Colo., 1972 (unpublished); R. L. Elgin, thesis (California Institute of Technology, 1973) (unpublished).

⁶G. A. Stewart, S. Siegel, and D. L. Goodstein, in *Ref. 5*.

⁷A. D. Novaco, *Phys. Rev. A* **7**, 1653 (1973).

⁸D. E. Beck, *Mol. Phys.* **14**, 311 (1969).

⁹W. L. Taylor and S. Weissman, *J. Chem. Phys.* **55**, 4000 (1971); J. M. Farrar and Y. T. Lee, *J. Chem. Phys.* **56**, 5801 (1972).

¹⁰M. Schick and C. E. Campbell, *Phys. Rev. A* **2**, 1591

(1970).

¹¹W. M. Gersbacher, Jr., and F. J. Milford, *J. Low Temp. Phys.* **9**, 189 (1972).

¹²H. R. Glyde and F. C. Khanna, *Can. J. Phys.* **50**, 1143 (1972).

¹³The function $\bar{v}(r)$ is just the exponential repulsion of the Beck potential.

¹⁴L. H. Nosanow, *Phys. Rev.* **146**, 120 (1966).

¹⁵R. A. Guyer, in *Solid State Physics*, edited by F. Seitz, D. Turnbull, and H. Ehrenreich (Academic, New York, 1969), Vol. 23.

¹⁶B. H. Brandow, *Ann. Phys. (N.Y.)* **74**, 112 (1972).

¹⁷G. A. Stewart (private communication).

¹⁸J. G. Dash (private communication).

¹⁹A. Scharm, in *Adsorption-Description Phenomena*, edited by F. Ricca (Academic, New York, 1972).

²⁰C. E. Campbell and M. Schick, *Phys. Rev. A* **5**, 1919 (1972).